Raman Spectroscopy of Carbon Materials: Structural Basis of Observed Spectra

Yan Wang, Daniel C. Alsmeyer, and Richard L. McCreery*

Department of Chemistry, The Ohio State University, 120 W. 18th Ave., Columbus, Ohio 43210

Received April 17, 1990

The first- and second-order Raman spectral features of graphite and related sp^2 carbon materials were examined with laser wavelengths ranging from 293 to 1064 nm. A wide range of carbon materials was considered, including highly ordered pyrolytic graphite (HOPG), powdered and randomly oriented graphite, and glassy carbon prepared at different heat-treatment temperatures. Of particular interest is boron-doped highly ordered pyrolytic graphite (BHOPG), in which boron substitution decreases local lattice symmetry but does not disrupt the ordered structure. New second-order bands at 2950, 3654, and ~4300 cm^{-1} are reported and assigned to overtones and combinations. The D band at 1360 cm^{-1}, which has previously been assigned to disordered carbon, was observed in ordered boronated HOPG, and its overtone is strong in HOPG. The observed Raman shift of the D band varies with laser wavelength, but these shifts are essentially independent of the type of carbon involved. It is concluded that the D band results from symmetry breaking occurring at the edges of graphite planes in sp^2 carbon materials or at boron atoms in BHOPG. The observations are consistent with the phonon density of states predicted for graphitic materials, and the fundamental and higher order Raman features are assignable to theoretically predicted lattice vibrations of graphite materials. The laser wavelength dependence of the D band frequency appears to result from scattering from different populations of phonons, perhaps through a resonance enhancement mechanism. However, the results are inconsistent with resonance enhancement of graphite microcrystallites of varying size.

Introduction

The lattice dynamics and vibrational spectroscopy of sp^2 carbon materials have been the subject of numerous investigations, and representative references are included here.[1-20] Raman spectroscopy has been an important tool in such investigations, because the Raman spectrum is particularly sensitive to the microstructure of the carbon. The *a*- and *c*-axis coherence lengths, L_a and L_c, and the d_{002} interplanar spacing all affect the Raman spectrum of graphitic materials, thus providing useful diagnostics for carbon structure and properties.[1,5,7,9,17] Despite the significant research effort invested by many laboratories on understanding the Raman spectroscopy of graphitic materials, the assignments and behavior of several Raman spectral features remain unclear. Our own laboratory has correlated the Raman spectroscopy of sp^2 carbon materials with their electrochemical behavior[16,21,22] and the same questions arise about the structural basis of Raman features. The current work was initiated to provide new information about the physical basis of the observed Raman spectra, with particular emphasis on relationships of Raman spectra with carbon microstructure.

Single crystal graphite belongs to the D^4_{6h} symmetry group, and vibrational modes are of the types $2E_{2g}$, $2B_{2g}$, E_{1u}, and A_{2u},[1,3,5,12,19] shown in Figure 1. The two E_{2g} modes are Raman active and have been identified with the Raman band at 1582 cm^{-1} and a low-frequency neutron scattering feature at 47 cm^{-1}, while the E_{1u} (1588 cm^{-1}) and A_{2u} (868 cm^{-1}) are IR active and observable with IR reflectance.[14] The B_{2g} modes are optically inactive, but one has been observed by neutron scattering at 127 cm^{-1}. Highly ordered pyrolytic graphite (HOPG) exhibits only the 1582-cm^{-1} band in the fundamental region between 1100 and 1700 cm^{-1},[1] but also shows second order features between 2400 and 3300 cm^{-1}.[5,9,23] Nemanich and Solin have attributed the strong feature at ca. 2720 cm^{-1} and weaker peaks at ~2450 and 3248 cm^{-1} to overtones of fundamental modes and accounted for their presence using phonon dispersion relationships.[5] On the basis of theoretical calculations of the phonon density of states, Al-Jishi and Dresselhaus[20,23] have attributed the second-order bands

Table I. Reported Vibrational Modes for Graphitic Carbon Materials

carbon type	$\Delta\bar{\nu}$, cm^{-1}	rel int[a]	assgnt	ref
natural single crystal	1575	vs	E_{2g}	1
HOPG	1581	vs	E_{2g}	5
HOPG	1582	vs	E_{2g}	3
HOPG	1582	vs	E_{2g}	15
HOPG	127	w	B_{2g}	2, 41
HOPG	42	w	E_{2g}	2
HOPG	868	IR only	A_{2u}	14
HOPG	1588	IR only	E_{1u}	14
HOPG	~1620	s	E'_{2g}	42
HOPG	3248	vw	2×1624 cm^{-1}	5
HOPG	2710	s	2×1355 cm^{-1}	5
HOPG	~2450	w	2×1225 cm^{-1}?	5
HOPG, ion implanted	2970	vw	E'_{2g} + D	24
glassy carbon	1582–1600[b]	vs	E_{2g}	9, 17
GC-20	1605	vs	E_{2g}	16
GC	1355[c]	vs	A_{1g}	1
GC	1360[c]	vs	A_{1g}	16
GC	1355[c]	vs	D	5
GC, PG, HOPG	2640–2732[c]	s	2×1360	7
GC, PG	1320–1360[c]	s	D	7

[a] vs = very strong, s = strong, w = weak, vw = very weak. [b] Depends on heat-treatment temperature. [c] Depends on λ_0.

* Author to whom correspondence should be addressed.

(1) Tuinstra, F.; Koenig, J. L. *J. Chem. Phys.* **1970**, *53*, 1126.
(2) Nicklow, R.; Wakabayashi, N.; Smith, H. G. *Phys. Rev. B* **1972**, *5* 4951.
(3) Nemanich, R. J.; Lucovsky, G.; Solin, S. A. *Mater. Sci. Eng.* **1977**, *31*, 157.
(4) Mani, K. K.; Ramani, R. *Phys. Status Solidi* **1974**, *61*, 659.
(5) Nemanich, R. J.; Solin, S. A. *Phys. Rev. B* **1979**, *20*, 392.
(6) Nakamizo, M.; Kammereck, R.; Walker, P. L. *Carbon* **1974**, *12*, 259.
(7) Vidano, R. P.; Fischbach, D. B.; Willis, L. J.; Loehr, T. M. *Solid State Commun.* **1981**, *39*, 341.
(8) Nakamizo, M.; Tamai, K. *Carbon* **1984**, *22*, 197.
(9) Vidano, R.; Fischbach, D. B. *J. Am. Ceram. Soc.* **1978**, *61*, 13.
(10) Tsu, R.; Gonzales, J.; Hernandez, I. *Solid State Commun.* **1978**, *27*, 507.
(11) Dresselhaus, M. S.; Dresselhaus, G. *Adv. Phys.* **1981**, *30*, 139.
(12) Reference 11, pp 290–298.

0897-4756/90/2802-0557$02.50/0

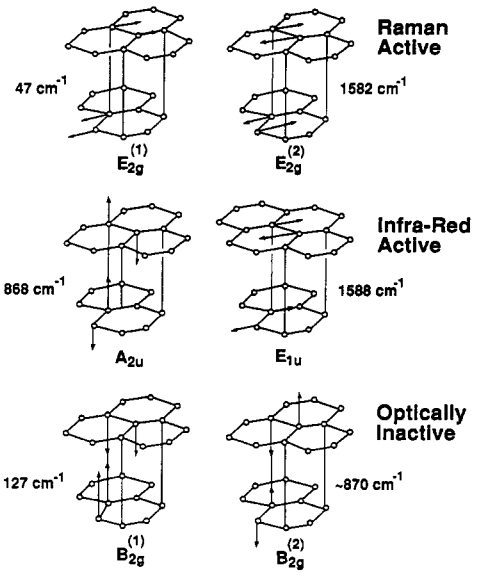

Figure 1. Vibrational modes for single-crystal graphite. Drawings were adapted from ref 3; vibrational assignments are from refs 3, 5, and 20. The $B_{2g}^{(2)}$ frequency is predicted but not yet observed experimentally.

at ~2450, 2730, and 3248 cm^{-1} to overtones of Raman-forbidden fundamentals, with good agreement between predicted and observed second order peaks. They have also theoretically predicted the dependence of fundamental intensities on L_a for partially graphitized carbon, on the basis of breakdown of the wave vector selection rule.[18] The HOPG spectrum will be discussed in more detail below, but one can conclude from the available literature that the assignments for known Raman features in pristine HOPG are uncontroversial. Representative frequencies and assignments for carbon vibrational features from the literature are listed in Table I.

The spectrum changes significantly for finite-sized microcrystallites (L_a < 1000 Å), and the origin of the changes is not clear.[1,5,6,17,23,25,26] The most obvious effect is the appearance of a band at ca. 1360 cm^{-1} with the 1360 cm^{-1}/1582 cm^{-1} intensity ratio (I_{1360}) increasing with decreasing microcrystallite size.[1] The empirical linear relationship between $1/L_a$ and I_{1360} is a useful means to determine the average L_a for a given carbon sample. The reasons for the appearance of the ~1360-cm^{-1} band for finite L_a are quite controversial.[5,13,24-26] Several workers have attributed it to a decrease in symmetry near microcrystallite edges, reducing the symmetry from D_{6h} to C_{3v} or even C_s.[1,25,27] New vibrational modes of the lattice may then become active, such as an A_{1g} mode proposed by Tuinstra and Koenig.[1] A related mechanism is breakdown of the $\vec{k} = 0$ selection rule for optical phonons near crystallite edges.[1,2,5,23,24] Such breakdown permits phonons other than 1582 and 47 cm^{-1} to become active, and the spectra reflect the density of phonon states in the lattice. A very different explanation for the 1360-cm^{-1} mode is the existence of specific vibrations at the edges, e.g., oxides or C=C groups which are present only at the edge.[25] Unlike the proposed A_{1g} mode, these edge vibrations are not directly related to the hexagonal graphite lattice but are analogous to functional groups. All reports concur that the 1360-cm^{-1} mode is related to structural disorder (and it will be referred to as the D band hereafter), but there is not a clear consensus on its origin.

A further complication of the D band is its unusual dependence on laser wavelength λ_0.[7,19,25] Vidano et al. reported that the position ($\Delta\bar{\nu}$) of the D band shifted from 1360 to 1330 cm^{-1} when λ_0 was increased from 488 to 647 nm,[7] and several possible explanations for this effect have been proposed. Variations in λ_0 will change the Raman sampling depth, possibly leading to variation in the spectrum if the carbon structure varies with depth.[25] Alternatively, the D band may be resonance enhanced, so that different subpopulations of crystallites (with different $\Delta\bar{\nu}$) may be sampled at different λ_0.[7] Polyacetylene exhibits such behavior,[28,29] and perhaps graphite is acting like a two-dimensional analogue of the linear system. A similar effect has been observed in quasi-one-dimensional crystals of halogen bridged platinum complexes, where the dependence of Raman shift on laser wavelength was attributed to resonance enhancement of subpopulations of the crystal having different vibrational frequencies.[30-33]

In the current work, we sought to clarify some of these controversial issues by three different approaches. First, the variety of carbon samples was expanded over previous investigations, to include HOPG, pyrolytic graphite, powdered graphite, polished glassy carbon (heat treated at 1000, 2000, and 3000 °C), and the fractured face of glassy

Table II

λ_0, nm	laser[a]	spectrometer[b]	detector	ref
292.8	QCW[c]	ISA 640	CCD[d]	40
350.7	Kr^+	Spex 1403	PMT (RCA 31034)	36, 37
406.7	Kr^+	Spex 1403	PMT	36, 37
457.9–514.5	Ar^+	Spex 1403	PMT	36, 37
568.2	Kr^+	Spex 1403	PMT	36, 37
647.1	Kr^+	Spex 1403	PMT	36, 37
782	Diode	ISA 640	CCD	38, 39
1064	YAG[e]	interferometer[e]	germanium[e]	34

[a] Kr^+ was a Coherent Model 100; Ar^+ was a Coherent 90-5; the diode laser was Liconix "Diolite" AlGaAs. [b] Spex 1403 is an additive dispersion double monochromator; ISA 640 is a 640 mm single spectrograph. [c] Quasi-CW YAG pumped dye laser; see ref 32. [d] Charge couple device array detector. [e] Located at DuPont, Wilmington, DE; see refs 26 and 27.

(13) Knight, D. S.; White, W. B. *J. Mater. Res.* **1989**, *4*, 385.
(14) Nemanich, R. J.; Lucovsky, G.; Solin, S. A. *Solid State. Commun.* **1977**, *23*, 117.
(15) McQuillan, A. J.; Hester, R. E. *J. Raman Spectrosc.* **1984**, *15*, 15.
(16) Bowling, R. J.; Packard, R. T.; McCreery, R. L. *J. Am. Chem. Soc.* **1989**, *111*, 217.
(17) Lespade, P.; Marchand, A.; Couzi, M.; Cruege, F. *Carbon* **1984**, *22*, 375.
(18) Lespade, P.; Al-Jishi, R.; Dresselhaus, M. S. *Carbon* **1982**, *20*, 427.
(19) Baranov, A. V.; Bekhterev, A. N.; Bobovich, Y. S.; Petrov, V. I. *Opt. Spectrosc. (USSR)* **1987**, *62*, 613.
(20) Wagner, J.; Ramsteiner, M.; Wild, C.; Koidl, P. *Phys. Rev. B* **1989**, *40*, 1817.
(21) Bowling, R.; Packard, R. T.; McCreery, R. L. *Langmuir* **1989**, *5*, 683.
(22) Rice, R. J.; McCreery, R. L. *Anal. Chem.* **1989**, *61*, 1637.
(23) Al-Jishi, R.; Dresselhaus, G. *Phys. Rev. B* **1982**, *26*, 4514.
(24) Elman, B. S.; Dresselhaas, M. S.; Dresselhaas, G.; Maby, E. W.; Mazurek, H. *Phys. Rev. B* **1981**, *24*, 1027.
(25) Mernagh, T. P.; Cooney, R. P.; Johnson, R. A. *Carbon* **1984**, *22*, 39.
(26) Katagiri, G.; Ishida, H.; Ishitani, A. *Carbon* **1988**, *26*, 565.
(27) Fateley, W. G.; Dollish, F. R.; McDevitt, N. T.; Bentley, F. F. *Infrared and Raman Selection Rules for Molecular and Lattice Vibrations*; Wiley Interscience: New York, 1972; pp 162–164.
(28) Schugerl, F. B.; Kuzmany, H. *J. Chem. Phys.* **1981**, *74*, 953.
(29) Kuzmany, H. *Pure Appl. Chem.* **1985**, *57*, 235.
(30) Conradson, S. D.; Dallinger, R. F.; Swanson, B. I.; Clark, R. J. H.; Croud, V. B. *Chem. Phys. Lett.* **1987**, *135*, 463.
(31) Tanaka, M.; Kurita, S.; Kojilma, T.; Yamada, Y. *Chem. Phys.* **1984**, *91*, 257.
(32) Tanaka, M.; Kurita, S. *J. Phys. C: Solid State Phys.* **1986**, *19*, 3019.
(33) Clark, R. J. H.; Karmoo, M. *J. Chem. Soc., Faraday Trans. 2* **1983**, *79*, 519.

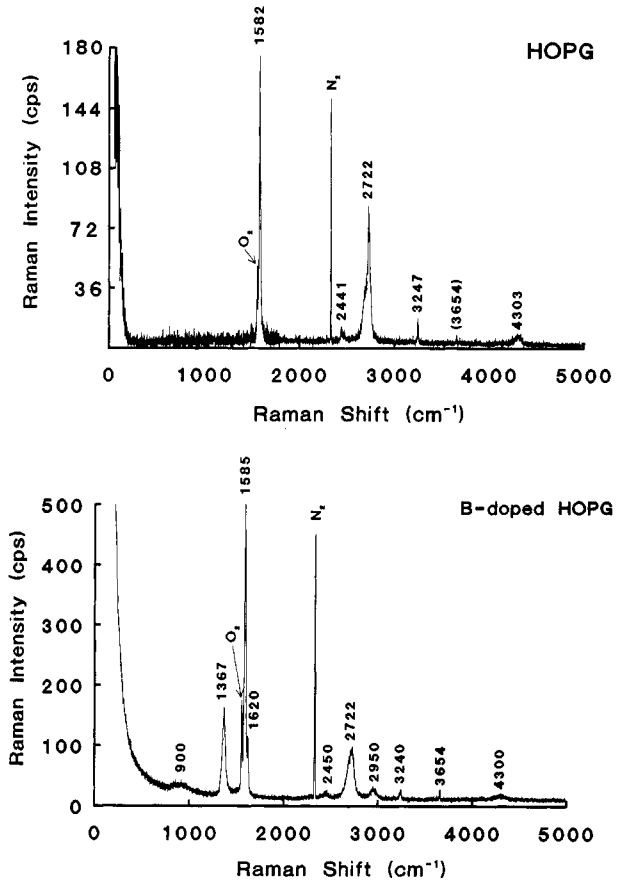

Figure 2. Raman spectra of graphite materials with λ_0 = 515 nm. Laser power at the sample was 50 mW; spectral resolution, 5 cm^{-1}. The upper spectrum is basal plane HOPG; the lower is basal plane B-doped HOPG.

carbon. Second, the range of laser wavelengths was broadened to 293–1064 nm. Third, HOPG doped with 0.5% boron was examined in detail.

Experimental Section

All Raman spectra were obtained in air at room temperature. With the exception of the 1064-nm laser, laser power at the sample was kept below 50 mW to minimize sample heating. The 1064- and 293-nm spectra were obtained with backscattered geometry,[26,27,32] but all others used a 55–75° incidence angle (relative to surface normal), with the incident electric field polarized parallel to the sample surface unless noted otherwise. Raman scattering was collected along a direction nearly normal to the sample surface. To cover a wide laser wavelength range, a variety of laser and spectrometer combinations were employed, as listed in Table II.[34-40] Although a correction for quantum efficiency variations with wavelength among the various detectors was not attempted, the D and E_{2g} mode frequencies are close enough to each other that variation in intensity ratios from quantum efficiency variation was small.

HOPG and BHOPG were obtained from Union Carbide; glassy carbon grades GC10, GC20, and GC30 (1000, 2000, 3000 °C heat treated) from Tokai; pyrolytic graphite from Pfizer; graphite powder from Ultracarbon, grade UCP-1-M; and graphite rod from Zeebac (grade HP-242,A1). Fractured GC-20 surfaces were obtained by fracturing a 3-mm-diameter rod with no additional treatment. The remaining GC surfaces were polished with 0.05-μm alumina to a mirrorlike finish. HOPG basal plane and BHOPG were freshly cleaved before each spectrum was obtained. HOPG edge plane was prepared by the method of Katagiri,[26] involving polishing followed by 600 °C heat treatment for 1 h in argon.

Table III. Peak Position, $\Delta\bar{\nu}$ (cm^{-1}), of Basal Plane Graphite for λ_0 = 458 and 515 nm

HOPG		BHOPG		
458 nm	515 nm	458 nm	515 nm	assgnt
		none[a]	(~900)[b]	A_{2u}
(1365)[c]	(1350)[c]	1380	1367	D
1577	1582 (1579)[c]	1591	1585	E_{2g}
		none[a]	1620	E'_{2g}
	2441	2440	2450	2 × 1220 cm^{-1}
2746	2722 (2717)[c]	2753	2722	2D
		2974	2950	E_{2g} + D
3246	3247	3242	3240	2 × E'_{2g}
		3653	3654	3 × 1220 cm^{-1}
(~4340)[c]	4303	(~4309)[b]	(~4300)[b]	2D + E_{2g}

[a] Not observable or unresolved. [b] Approximate due to a broad peak. [c] Determined on the edge plane of HOPG.

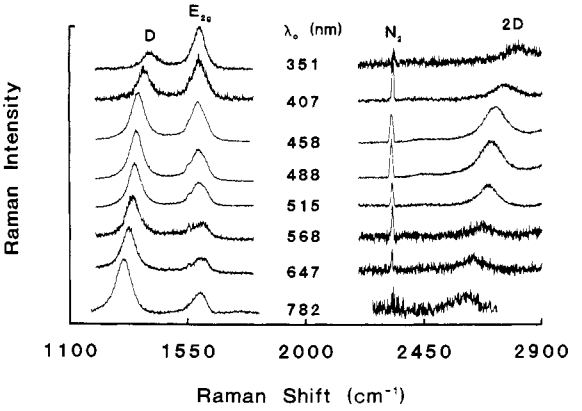

Figure 3. Raman spectra of polished GC-20 at different laser wavelengths (λ_0). Laser power at the sample ranged from 20 to 60 mW; spectral resolution was 4–10 cm^{-1}.

Results

A Raman spectrum of HOPG over a wide $\Delta\bar{\nu}$ range is shown in Figure 2. In addition to the previously reported peaks at 1582, 2441, 2722, and 3247 cm^{-1}, there is a high-frequency peak at ~4303 cm^{-1}. A spectrum of 0.5% boron-doped HOPG is shown in Figure 2 as well. Hagio et al.[43,44] showed that boron doping to 0.6% had only minor effects on the X-ray diffraction parameters, with d_{002} decreasing from 3.354 to 3.351 Å and a_0 increasing from 2.461 to 2.464 Å. L_a and L_c remained large upon boron doping, on the basis of X-ray diffraction line widths. However, they noted a strong 1360-cm^{-1} Raman peak in BHOPG, indicating activity of additional phonons due to symmetry breaking.[44] The new peaks observed in the BHOPG spectrum are listed in Table III. Apparently the breakdown in symmetry caused by randomly arranged boron atoms permits observation of more modes, including some that are rarely observed for any other type of sp^2 carbon. The infrared reflectance spectra for HOPG and BHOPG were obtained by using a conventional FTIR spectrometer and a gold mirror as a reference. HOPG exhibited a

(34) Chase, D. B. *J. Am. Chem. Soc.* **1986**, *108*, 7485.
(35) Chase, D. B. *Anal. Chem.* **1987**, *59*, 881A.
(36) Packard, R. T.; McCreery, R. L. *Anal. Chem.* **1987**, *59*, 2692.
(37) McCreery, R. L.; Packard, R. T. *Anal. Chem.* **1989**, *61*, 775A.
(38) Williamson, R.; Bowling, R. J.; McCreery, R. L. *Appl. Spectrosc.* **1989**, *43*, 372.
(39) Wang, Y.; McCreery, R. L. *Anal. Chem.* **1989**, *61*, 2647.
(40) Gustafson, T. L.; Palmer, J. F.; Roberts, D. M. *Chem. Phys. Lett.* **1986**, *127*, 505.
(41) Dolling, G.; Brockhouse, B. N. *Phys. Rev.* **1962**, *128*, 1120.
(42) Underhill, C.; Leung, S. Y.; Dresselhaus, G.; Dresselhaus, M. S. *Solid State Commun.* **1979**, *29*, 769.
(43) Hagio, T.; Nakamizo, M.; Kobayashi, K. *Carbon* **1987**, *25*, 637.
(44) Hagio, T.; Nakamizo, M.; Kobayashi, K. *Carbon* **1989**, *27*, 259.

Table IV. Peak Positions and Line Widths of Raman Bands for Carbon Materials, λ_0 = 458 nm

graphitic material	D, cm^{-1}	fwhm,[a] cm^{-1}	E_{2g}, cm^{-1}	fwhm, cm^{-1}	peak ratio,[b] D/E_{2g}	2D peak position, cm^{-1}	3240-cm^{-1} peak posn, cm^{-1}
HOPG (basal)	none	none	1577	20	0.00	2746	3246
HOPG (edge)	1365	41	1577	20	0.18	2746	3246
PG (basal)[c]	1365	41	1577	22	0.21	2732	3246
PG (edge)	1361	33	1577	23	0.22	2728	3241
graphite rod	1365	62	1573	34	0.23	2737	3241
graphite powder	1360	43	1573	34	0.33	2728	3232
GC-30S	1363	47	1583	54	0.53	2724	3237
fractured GC-20S	1360	46	1582	51	0.50	2725	3232

[a] Full width at half-maximum. [b] Integrated peak intensity ratio. [c] Pyrolytic graphite.

Table V. Peak Positions and Line Widths of Raman Bands for Carbon Materials, λ_0 = 515 nm

graphitic materials	D, cm^{-1}	fwhm,[a] cm^{-1}	E_{2g}, cm^{-1}	fwhm,[a] cm^{-1}	peak ratio[b] D/E_{2g}	2D peak posn, cm^{-1}	~3240-cm^{-1} peak posn	L_a from ref 1, Å
HOPG (basal)	none	none	1582	18	0.00	2722	3243	>1000
HOPG (edge)	1354	33	1579	18	0.25	2717	3243	170
PG (basal)	1352	31	1577	25	0.15	2706	3245	260
PG (edge)	1352	34	1577	24	0.30	2706	3245	140
graphite rod	1347	42	1573	21	0.78	2705	3245	53
graphite powder	1352	43	1580	30	0.98	2699	3240	42
GC-30S	1347	47	1586	70	1.13	2699	3234	37
fractured GC-20S	1350	53	1584	64	1.22	2696	3232	32

[a] Full width at half-maximum. [b] Integrated peak intensity ratio.

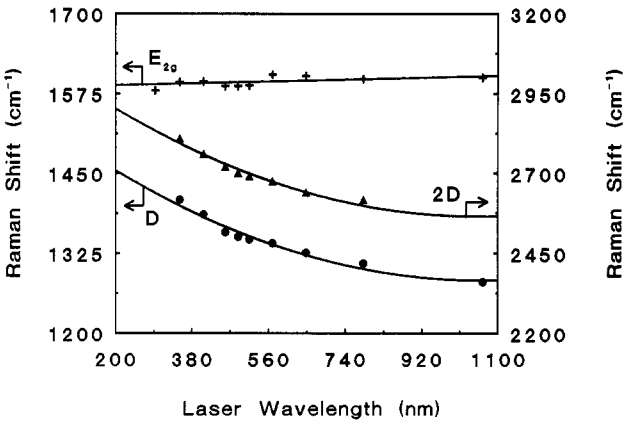

Figure 4. Plot of D, 2D, and E_{2g} Raman peak positions for polished GC-20 as functions of laser wavelengths.

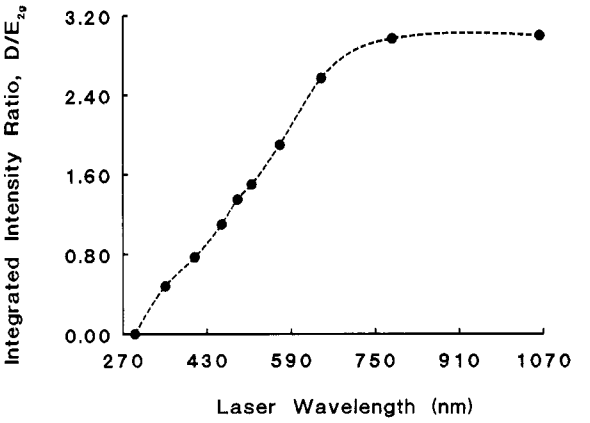

Figure 5. Ratio of integrated D peak intensity to integrated E_{2g} intensity as a function of λ_0. Sample was polished GC-20 in all cases.

well-defined feature at 1589 cm^{-1} and a very weak peak at 868 cm^{-1}, similar to those reported by Nemanich et al.[3] For BHOPG, the high-frequency feature was at 1591 cm^{-1}, and an 868-cm^{-1} feature was not observed. However, BHOPG exhibited a broad but discernible peak at ca. 1250 cm^{-1} that was not evident for HOPG.

Table III also includes peak position results for 458-nm excitation, revealing that the 1360-, 2722-, 2950-, and possibly the ~4300-cm^{-1} peaks shift to higher $\Delta\nu$ with decreasing λ_0, while the other peaks remain nearly stationary. This effect is shown in more detail for the D, E_{2g}, and ~2700-cm^{-1} peaks of GC in Figure 3. As shown in Figures 3 and 4 the E_{2g} peak position is almost independent of λ_0, but the 1360- and ~2700-cm^{-1} bands shift substantially, with the 2700-cm^{-1} band shift about twice as large. These observations are consistent with those of Vidano and Fischbach[7] and Baranov et al.,[19] but over a wider wavelength range. There is significant variation in relative intensities of the 1360- and 1582-cm^{-1} bands with λ_0; I_{1360} increases by about a factor of 5 between λ_0 = 351 and 1064 nm (Figure 5). The D peak was below the noise level for λ_0 = 293 nm, where its area was less than 20% of the E_{2g} area. A similar but much smaller effect has been reported for Graphon carbon black over a 458–647-nm λ_0 range.[25]

Raman peak positions for eight different carbon samples and four laser wavelengths are shown in Tables IV–VI. All eight samples were examined with 458- and 515-nm light, and the D, E_{2g}, and 2700-cm^{-1} bands were examined at 407 and 782 nm as well. As shown graphically in Figure 6, the position of the D band is nearly independent of the carbon material, even though L_a ranges from ca. 24 to >1000 Å. The D position *does* depend on λ_0 in the same way for a variety of carbon materials, and thus λ_0 determines the D-band position, *not* L_a. Also note that the D/E_{2g} intensity ratio does depend on carbon type, as expected from early correlations of Raman and X-ray diffraction results.[1] This peak ratio at λ_0 = 515 nm was used to establish the x-axis scale in Figure 6. It is also apparent from Tables IV–VI and Figure 6 that the E_{2g} frequency shifts up and its line width increases as the carbon becomes less ordered (i.e., smaller L_a).

There has been some discussion in the literature about the association of the D band with microcrystallite size or with crystallite edges.[1,17,25,26] Since smaller microcrystallites

Table VI. D, E_{2g}, and 2D Frequencies for λ_0 = 407–782 nm

	λ_0			
	407	458	515	782
		BHOPG Basal		
D	1394	1380	1367	1330
E_{2g}	1585	1591	1585	1593
2D	2773	2753	2722	*a*
		HOPG Edge		
D	1378	1365	1354	1305
E_{2g}	1583	1577	1579	1585
2D	2763	2746	2717	*a*
		PG Basal		
D	1383	1365	1352	1312
E_{2g}	1582	1577	1577	1575
2D	2773	2732	2706	*a*
		Graphite Rod		
D	1378	1365	1347	1310
E_{2g}	1582	1573	1573	1580
2D	2768	2737	2705	*a*
		Graphite Powder		
D	1385	1360	1352	1313
E_{2g}	1588	1573	1580	1575
2D	2771	2728	2699	*a*
		GC-20S		
D	1386	1358	1347	1310
E_{2g}	1594	1587	1588	1598
2D	2762	2722	2692	2618

[a] Not observed, due to poor quantum efficiency of CCD in this wavelength region.

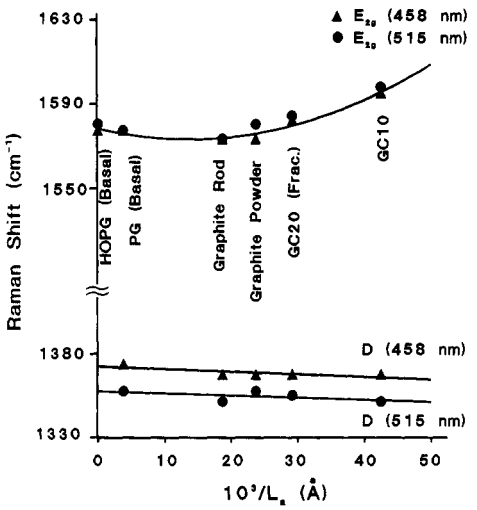

Figure 6. Plot of D and E_{2g} peak positions of different carbon materials as a function of the reciprocal of crystalline layer size L_a at two laser wavelengths. L_a was determined from peak intensity ratio as in ref 1.

will have a greater edge density, the question arises of whether D intensity implies smaller microcrystallites or merely the presence of edges. Katagiri approached this issue by obtaining Raman spectra of the edge plane of PG.[26] The spectra were strongly sensitive to the polarization of the laser light relative to the graphite planes, indicating that the edge consisted of primarily the oriented edges of relatively large crystallites. If the D band arises from small microcrystallites only, it should not be present on the HOPG edge plane. Katagiri's results on PG are confirmed for the more ordered HOPG by Figure 7, which shows HOPG edge plane spectra at two laser wavelengths. For both λ_0, the strong dependence of intensity on polarization implies that the sample is ordered, with minor contributions from residual disordered particles resulting from preparation. Furthermore, the edge plane D bands

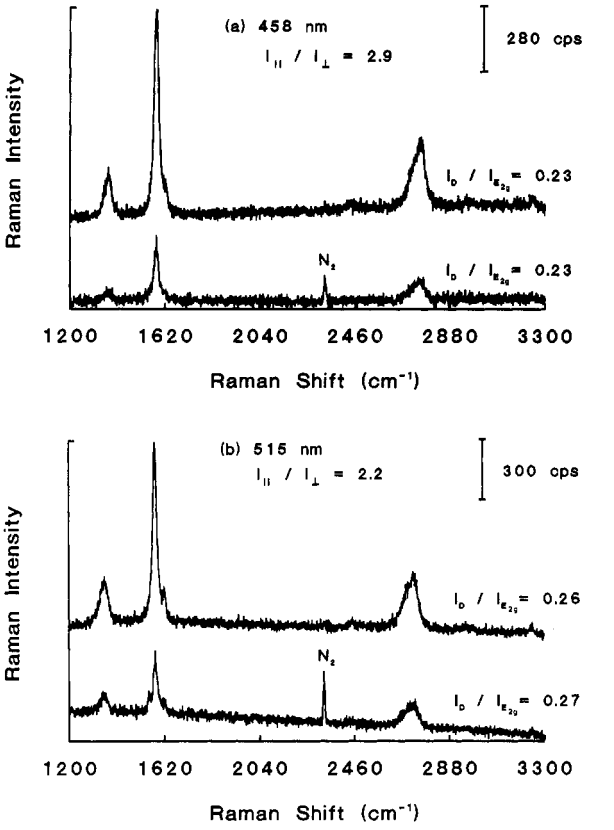

Figure 7. Polarized Raman spectra of edge plane HOPG with λ_0 = 458 (a) and 515 nm (b). Laser power at the sample was 40 mW; spectral resolution, 10 cm^{-1}. The upper spectra were measured with the incident laser radiation polarized parallel to the *a* axis of HOPG, and the lower spectra with laser light polarized parallel to the *c* axis.

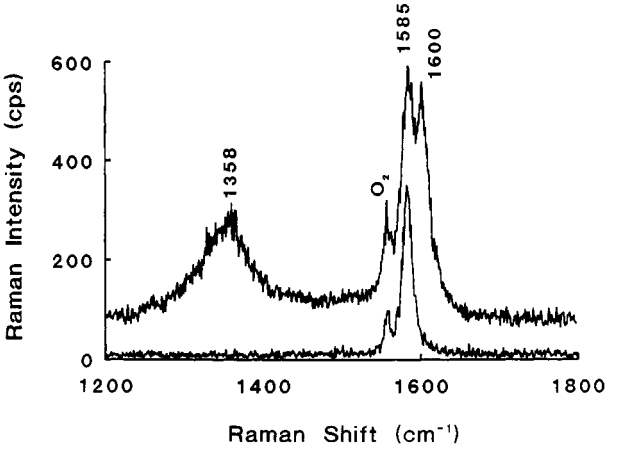

Figure 8. Effect of electrochemical pretreatment (ECP) on the Raman spectrum of basal plane HOPG at 515 nm. The lower spectrum was the initial HOPG surface before ECP and the upper spectrum was after 2 min of anodization at 2.0 V vs Ag/AgCl in 0.1 M KNO_3, and then 30 s at −0.1 V vs Ag/AgCl. Laser power at the sample was 20 mW; resolution was 5 cm^{-1}.

exhibit the same shift with λ_0 as observed for other carbon samples such as GC, powdered graphite, etc. If the D band arises from small microcrystallites, it should not be observed for the oriented edges of large (>1000 Å) crystallites on HOPG edge plane.

A further confirmation of edge plane behavior is provided by electrochemical oxidation of basal plane HOPG. Such treatment causes damage to the basal plane by formation of surface oxides, and lattice damage appears to occur along relatively straight paths, resulting in large

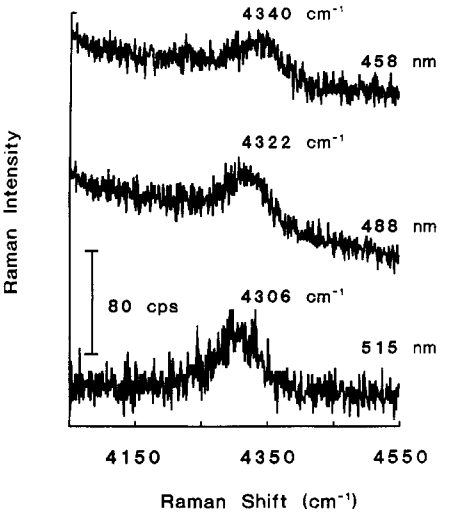

Figure 9. Third-order Raman spectra of basal plane HOPG at three different laser wavelengths. Laser power at the sample was 20–40 mW; resolution was 4–5 cm^{-1}.

crystallites with oxidized edges.[16,21] The Raman spectrum of the oxidized basal plane shown in Figure 8 exhibits a D band with the same position as other carbon materials, depending only on λ_0. The edge defects formed during electrochemical oxidation contain many oxygen functional groups and are likely to differ greatly in chemical composition from the edges present in GC and other disordered carbons. However, the same D-band position is observed after oxidation, demonstrating that the quite different chemistry on the oxidized edge has no observable effect on the D frequency.

The dependence of the D, E_{2g}, and ~2700-cm^{-1} intensities on λ_0 was examined by using Na_2SO_4 as an internal standard. Mixtures of graphite powder and Na_2SO_4 were pressed into a pellet and spectra were obtained for λ_0 = 407–782 nm. The ratio of the three carbon band intensities to that of the SO_4^{2-} band at 1160 cm^{-1} changed by less than a factor of 3 over the λ_0 range employed. This observation is consistent with that of Mernagh et al., who noted that none of the three bands changed in intensity by more than a factor of 2 between 458 and 647 nm.[25]

Finally, the weak feature at ca. 4300 cm^{-1} in HOPG is shown in more detail in Figure 9. The peak position shifts to lower frequency with increasing λ_0, similar to the ca. ~2700-cm^{-1} band.

Discussion

The conclusions available from the current results will be grouped into three general areas: the assignments of observed vibrational modes, the nature and origin of the D band at ~1360 cm^{-1}, and the effects of λ_0 on observed spectra. An important factor in the interpretation of the Raman spectrum is the phonon dispersion relation and density of states predicted for graphite.[2,20,34] Although only the phonons with E_{2g} symmetry are predicted to be Raman active in an infinite graphite crystal, the entire population distribution of phonons as a function of frequency is available from the density of states calculation. The theoretical results of Nicklow et al.[2] and Al-Jishi and Dresselhaus[23] are both consistent with the observed Raman features of HOPG with λ_0 = 515 nm.

Vibrational Mode Assignments. The introduction of boron into presumably random sites of HOPG has useful consequences for understanding the Raman spectroscopy of graphitic materials. Boron doping has been shown to be substitutional, with boron atoms occupying trigonal sites.[43,44] Presumably due to electronic effects, the d_{002} and a_0 spacing change very slightly, and the X-ray diffraction results for BHOPG are altered very little compared to HOPG. The absence of major changes in L_a and L_c with boron doping is consistent with substitutional doping with minor effects on crystallite size and no segregation of boron-containing phases. In contrast, the Raman spectrum of BHOPG shows new features compared to HOPG, with the 1367-, 1620-, and 2950-cm^{-1} bands being apparent in the ordered material, in addition to the expected bands at 1585, 2722, 2450, and 3240 cm^{-1}. Both HOPG and BHOPG exhibit previously unreported bands at 3654 and ~4300 cm^{-1}. We conclude that boron doping breaks the local symmetry of the graphite, permitting most vibrations predicted from the phonon dispersion relationships. Symmetry near a boron atom may be C_{3v}, which has A and E vibrations that are Raman active,[25] or C_s. Since the hexagonal graphite lattice is largely undisturbed by boron substitution, the vibrational frequencies are similar to HOPG, but more are optically active. Therefore, we assign the ~900-cm^{-1} band to A_{2u} (as observed at 868 cm^{-1} in HOPG by IR reflectance), the 1585-cm^{-1} band to E_{2g}, and the 1620-cm^{-1} band to E'_{2g}. Although 1620 cm^{-1} corresponds to a peak in the density of states for graphite,[5,23] a distinct 1620-cm^{-1} Raman band has previously been observed only for intercalation compounds and oxidized sp^2 carbon.[6,12,16] Dresselhaus et al.[12,42,45] assign the 1620-cm^{-1} band to an E_{2g} mode for a graphite "boundary" layer adjacent to an intercalant layer and not sandwiched between two other graphite planes. They attribute the upward frequency shift to differences in the electronic environment for the boundary layer compared to an inner layer. In the case of BHOPG, the 1620-cm^{-1} band (denoted here as E'_{2g}) is observable either because of the altered electronic environment near a boron atom or because of reduced symmetry.

The assignments of second-order peaks are facilitated by the λ_0 dependence of the D band. The ~2720-cm^{-1} band shifts with λ_0 at twice the rate of the D band, implying that ~2720 cm^{-1} is the first overtone of D, denoted 2D henceforth.[7] The 2950-cm^{-1} mode was observed only for BHOPG, and at both 458 and 515 nm, its frequency equaled the sum of the D and E_{2g} modes. Since there is no peak in the density of states at 1425 cm^{-1} (one-half of 2950 cm^{-1}), it seems unlikely that 2950 cm^{-1} is an overtone, implying that it is a combination, E_{2g} + D. This mode has been assigned as (E'_{2g} + D) in ion-implanted HOPG,[24] but the E_{2g} + D assignment here is more consistent with current results. The weak intensity of the 4300-cm^{-1} peak makes it difficult to accurately determine its position, but for HOPG, it appears to shift at about twice the rate of the D band (see Figure 9). A possible assignment is 2D + E_{2g}. The 2441-, 3247-, and 3654-cm^{-1} peaks observed for both HOPG and BHOPG are much less dependent on λ_0, implying no contribution from the D band. The assignment of 3242 cm^{-1} as (2 × 1620 cm^{-1}) was made originally by Nemanich and Solin.[5] A possibility for the 2441-cm^{-1} band is E_{2g} (1582 cm^{-1}) + A_{2u} (868 cm^{-1}), but this combination should not be Raman active in the D_{6h} symmetry group. Previous investigators have assigned this mode to (2 × 1220 cm^{-1}), where 1220 cm^{-1} corresponds to a peak in the calculated phonon density of states.[5,23] The latter assignment is supported by the observation of a small peak at 3654 cm^{-1}, which could be (3 × 1220 cm^{-1}), in both HOPG and BHOPG. The nature of the density of states peak at ~1220 cm^{-1} has been discussed by Al-

(45) Al-Jishi, R.; Dresselhaus, G. *Phys. Rev. B* **1982**, *26*, 4523.

Jishi and Dresselhaus,[23] and a weak 1250-cm^{-1} Raman feature has been observed in GC.[19] Although the ca. 1250-cm^{-1} feature in the IR reflectance spectra of BHOPG is broad and its frequency difficult to determine accurately, it may result from the ca. 1220-cm^{-1} fundamental.

For Raman spectroscopy of solutions and liquids, it is unusual to observe an overtone without observing the fundamental. Two conditions must be met for this to occur: the symmetry of the overtone must be the same as one of the polarizability elements, and the system must exhibit electrical or mechanical anharmonicity.[46,47] For the D_{6h} space group, even overtones contain A_{1g} and should be Raman allowed, even if the fundamental is not. So the anharmonicity of the graphite must be nonzero, and the 2444-, 2722-, and ~3242-, and 3654-cm^{-1} bands are attributable to overtones of forbidden fundamentals.

Nature of the D Band at ~1360 cm^{-1}. As noted above, the current results are consistent with the assignment of the D band to a high density of phonon states which are inactive unless the $\mathbf{k} = 0$ selection rule breaks down. From the observations of HOPG edge plane and electrochemically oxidized HOPG, it is clear that the $\mathbf{k}$ vector selection rule can break down near an edge of a large crystallite, and small (<1000 Å) microcrystallites are not necessary to observe the D band. Thus small L_a is a sufficient but not necessary condition for observing the D band. The D band clearly does not result from any chemical effects unique to the edge, such as oxides, isolated C=C bonds, or distinct vibrational modes. Major chemical changes to the edge, such as oxidation, produce no observable effects on the D frequency, and the same frequency is observed for a wide range of carbon materials at a given λ_0. Furthermore, the harmonic of the D band at ~2722 cm^{-1} is strongest for the most ordered graphite samples. Therefore the 1360-cm^{-1} band is a mode inherent in the graphite lattice, which becomes observable when symmetry is broken by an edge or a boron atom. The chemical composition of the edge or the size of the associated crystallite is unimportant to the frequency of the D band, but the presence of the edge permits scattering by the D band phonons.

In addition, variations in D-band position cannot be due to sampling depth. The frequency is the same for a variety of carbon materials and surface preparations, including pristine BHOPG basal plane and fractured GC. The latter two surfaces would not be expected to vary in structure with depth after a few atomic layers, yet the D-band frequency (and most others) is the same as that of other carbon materials, under conditions when the sampling depth is several hundred angstroms. Furthermore, the E_{2g} frequency is insensitive to λ_0 but does depend weakly on L_a (Figure 6). Thus if different L_a values existed at different depths, the E_{2g} frequency should vary with λ_0.

Dependence of the D Band on Laser Wavelength. The behavior of the D band for varying λ_0 is consistent with a hypothesis that subpopulations of phonons scatter different incident photons with different wavelengths. For example, short λ_0 (351 nm) is scattered preferentially by higher energy phonons, while long-λ_0 photons are scattered by lower energy, lower $\Delta\bar{\nu}$ phonons. The intensity of the D band relative to the E_{2g} band varies with carbon type because of varying edge density, but the position of the D band does not vary for different carbons. If the phonons that scatter are selected only by the incident λ_0, it will not matter what type of carbon is the host. The D-band frequency will depend only on incident λ_0, as is observed experimentally. Since the 2D-band position in HOPG also shifts with λ_0, the D-band frequency must be unrelated to microcrystallite effects. The variation in D-band intensity with λ_0 reflects the carbon microstructure, due to the variation in the extent of selection rule breakdown with edge density. Smaller microcrystallites (e.g., in GC) have higher D-band intensity than large crystallites (e.g., in HOPG) because there are more edges to break symmetry, but the same modes are observed in both cases. All results are consistent with different incident wavelengths sampling different phonon subpopulations.

A possible mechanism for sampling of subpopulations is resonance enhancement of finite-sized microcrystallites. This process is analogous to that observed for polyacetylene[29] and linear platinum halides,[30-33] in which a similar shift in $\Delta\bar{\nu}$ occurs with λ_0. The current results show that such a mechanism cannot be based on resonance enhancement of microcrystallites in graphite. In HOPG, with large crystallites that are presumably out of resonance with the laser light, the 2D band shows the same shift with λ_0. The $\Delta\bar{\nu}$ shift is independent of the degree of disorder, at odds with a mechanism based on microcrystallites. Thus the selection rule breakdown is fundamentally dependent on symmetry loss occuring near edges (or boron atoms), but the frequencies observed do not depend on crystallites or edges.

Although sampling of microcrystallite populations by resonance enhancement can be ruled out, it is still possible that resonance effects occur with the sp^2 lattice, as proposed by Baranov et al.[19] If resonance is involved, it differs substantially from conventional resonance Raman of small molecules. The D-band intensity does not vary greatly with λ_0 (by only a factor of 3–5),[25] and the D band is symmetric, unlike polyacetylene. Although intensity variations with λ_0 are difficult to measure due to uncertainties about an internal standard, it is clear that they do not vary by orders of magnitude. Whatever the mechanism of the effect, its result is scattering of different laser photons from phonons of differing energy.

In conclusion, the observed Raman spectra for a variety of carbon materials is consistent with the predicted phonon dispersion relations for hexagonal graphite, and all observed spectral peaks are assignable. The D-band intensity depends on edge density rather than microcrystallite size per se, and its frequency depends only on laser wavelength for a variety of carbon materials. Different laser wavelengths appear to sample different points along the phonon dispersion curve, but the selectivity is not attributable to resonance enhancement of different subpopulations of microcrystallites. Finally, the presence of the "disorder" bands of Raman spectra of sp^2 carbon is caused by reduced symmetry of the graphite lattice near edges or near a boron atom. The modes themselves are present but not Raman active in the ordered material.

Acknowledgment. We thank Prabir Dutta for many scientific discussions and technical assistance, Bruce Chase for obtaining the Raman spectrum of GC at 1064 nm, Terry Gustafson for spectra obtained at 293 nm, and Adina Enculescu for providing FTIR data on HOPG and BHOPG. In addition, we thank Bruce Bursten and Vladimir Bondybey for useful suggestions and Arthur Moore for the HOPG and BHOPG samples. The work was supported primarily by the Surface and Analytical Chemistry division of the National Science Foundation.

Registry No. C, 7440-44-0; B, 7440-42-8; graphite, 7782-42-5; polyacetylene, 25067-58-7.

(46) Long, D. A. *Raman Spectroscopy*; McGraw-Hill: New York, 1977; pp 78–81.
(47) Decius, J. C.; Hexter, R. M. *Molecular Vibrations in Crystals*, McGraw-Hill: New York, 1977; pp 267–270.